



Nonlinear backstepping control of a hydraulic simulator for reference road input

Referans yol girişi için hidrolik simülâtörün doğrusal olmayan geri-adımlamalı kontrolü

Muzaffer METİN^{1*}, Fırat Can YILMAZ², Göktürk TAŞAĞIL³, Timuçin BAYRAM³, Ferhat YİĞİT⁴

¹Department of Mechanical Engineering, Faculty of Mechanical Engineering, Yıldız Technical University, İstanbul, Türkiye.
mmetin@yildiz.edu.tr

²Department of Mechanical Engineering, Faculty of Engineering, Gebze Technical University, Kocaeli, Türkiye.
fcyilmaz@gtu.edu.tr

³Mert Teknik Incorporated, Research and Development Center, İstanbul, Türkiye.
gokturk.tasagil@mert.com, timucin.bayram@mert.com

⁴TIRSAN Trailer Industry and Trade Incorporated, Research and Development Center, Kocaeli, Türkiye.
ferhat.yigit@kaessbohrer.com

Received/Geliş Tarihi: 31.03.2023
Accepted/Kabul Tarihi: 06.05.2024

Revision/Düzeltilme Tarihi: 30.04.2024

doi: 10.5505/pajes.2024.67277
Research Article/Araştırma Makalesi

Abstract

In this paper, the problem of reference tracking was investigated for a road simulator system from the perspective of control theory. The suggested control signal is obtained from a nonlinear backstepping control algorithm. This design is used to mirror the road displacement signal in the test system containing a vehicle system that incorporates a hydraulic piston. The performance of the proposed controller is evaluated in the time and frequency domains, with the primary criterion being that the displacement of the test road irregularities created by the hydraulic piston is accurately reflected to the vehicle. Additionally, the frequency densities of the signals transmitted to the vehicle are expected to match the real road data. Real road signals for land vehicles are used as the reference input signals. We demonstrate the effectiveness of the control signal through the results obtained in a laboratory environment.

Keywords: Hydraulic system, Hydraulic road simulator, Backstepping control, Servo control.

Öz

Bu çalışmada, kontrol teorisi perspektifinden, yol simülâtör sistemi için referans takip problemi araştırılmıştır. Önerilen kontrol sinyali doğrusal olmayan bir geri adımlı kontrol algoritması üzerinden elde edilmiştir. Bu tasarım, hidrolik piston içeren bir taşıt sisteminden oluşan test sisteminde yol deplasman sinyalini yansıtmak için kullanılır. Önerilen kontrolcünün performansı zaman ve frekans alanlarında değerlendirilip, kontrol tasarımının temel gayesi hidrolik piston tarafından oluşturulan test yolu düzensizliklerinin yer değiştirmesinin araca doğru bir şekilde yansıtılmasıdır. Ayrıca, araca aktarılan sinyallerin frekans yoğunluklarının da gerçek yol sinyalleriyle eşleşmesi beklenmektedir. Kara taşıtları için gerçek yol verileri kontrol algoritmasındaki referans giriş sinyali olarak kullanılmıştır. Bir laboratuvar ortamında elde edilen sonuçlar üzerinden kontrol sinyalinin etkinliği gösterilmiştir.

Anahtar kelimeler: Hidrolik sistem, Hidrolik yol simülâtörü, Geri-adımlamalı kontrol, Servo kontrol.

1 Introduction

Transportation vehicles are always subjected to dynamic forces while in motion, due to the dynamic variables of the road they follow. Dynamic forces generated by road irregularities are transmitted to the body and suspension system of the vehicle from the wheels in land vehicles, while an aircraft system is subjected to pressure changes and other aerodynamic forces. Therefore, the parts of all transportation vehicles affected by dynamic forces are designed regarded to fatigue phenomena and the produced prototypes should be tested under realistic working conditions. These tests are often carried out with test rigs that simulate the realistic conditions in laboratory instead of the real road/terrain environment. These tests are generally carried out with test rigs that simulate realistic conditions in a laboratory environment, instead of simulating on actual road/terrain due to their advantages. Thus, tests that could operate for many hours on road/terrain can be done easily in a more controlled environment. Furthermore, test performed in

a laboratory environment minimizes the risk of working accidents due to the absence of drivers. These test systems generally operate with a hydraulic actuator due to their power and dynamic performance requirements. The performance and realistic working abilities of test systems are evaluated in the time and frequency domains. The reflection of the road irregularities measured from the road should be transferred to the vehicles realistically. At the same time, a matching is expected between the frequency density of these effects transmitted to the vehicle and actual road disturbances' frequency density. The performance of test systems depends on the technical specifications of the equipment and the algorithm that control the hydraulic actuators. The presence of factors such as parametric uncertainties, delays, sensor faults, and various nonlinearities turns the control of multi-axis fatigue simulator systems into a challenging and current problem to be solved in the automotive industry. Therefore, the fatigue durability of the vehicles should be investigated via the multi-axes servo-hydraulic test simulator system designed by

*Corresponding author/Yazışılan Yazar

researchers while the actual car working condition has been provided to the test rig. The time domain method approach to the test rig design is a simplifier when it is compared with the frequency domain method. The state space representation approach's applicability ability to the road simulator test control was presented at a small pick-up truck's life cycle durability test [1]. The use of an iterative approach in test rig simulations is a preferred method. In the case of tracking road data, the iterative method was utilized in the testing process on the poster rig [2]-[4]. It is recommended to investigate the development of a robust controller design that is capable of producing a signal that can accurately trace the road input signal in order to address the uncertain parameters present within the road simulator actuator [5]. The purpose of shaker test rigs for vehicles may differ from tracking the actual road disturbance input, such as modal analysis [6]. The platforms can possess a similar mathematical representation to the poster systems, which were operated by hydraulic systems. In the controller of the platforms like Stewart platform, an adaptive controller design [7,8], an internal model control [9], a high order differential feedback controller design [10], an acceleration identification algorithm development [11], an acceleration decoupling control [12], an optimal tuned cascade control strategy [13] were used in the literature. In the investigation of the strength of the material and the determination of the performance of the material, the usage of Model-predictive control (MPC) algorithm was researched and compared with Linear-quadratic regulator control method. It was found that the efficiency of the MPC becomes more dominant over Linear-quadratic-regulator (LQR) while the system constraints increase [14].

Extensive studies in literature have been conducted on the control of hydraulic systems. Hydraulic systems have been able to achieve position control through the implementation of PID controller designs, and achieve force control via PI, respectively [15]-[17]. A hybrid fuzzy-PID controller was designed for position control of the hydraulic system during the Bulk modulus parameter of the system that is variable [18]. Also, fault-tolerant control method usage has found an application area in the hydraulic system position control [19]-[21]. A fault-tolerant control algorithm was developed using a sliding adaptive controller, time delay estimation, and feedback linearization for the system with disturbances, uncertainties, and internal leakage faults [19]. A new friction model based on LuGre has been proposed for the purpose of friction compensation in an electrohydraulic servo system. The trajectory tracking performance of the proposed controller was evaluated using this improved friction model [22]. A recent approach to position control of electrohydraulic servo systems is model-based reinforcement learning, which involves the introduction of a control algorithm to enhance the control performance of hydraulic systems [23]. Unmeasurable system states could occur in the system control design. In this existence of the issue, a nonlinear adaptive output feedback robust control for the tracking of the desired trajectory at the system that has unknown matched and mismatched modeling, uncertainties, was investigated [24]. Adaptive controller designs at systems with parametric uncertainties were studied as another working area [25]-[27], a backstepping adaptive controller design for the aim of reference trace at the system was built successfully [28], an observer-based controller designs were used for controlling the hydraulic system [29]-[33], and an artificial neural network was

used for prediction of the chamber pressures in a hydraulic cylinder [34].

In this study, the proposed controller algorithm used in the single hydraulic valve system [35] is capable of generating real road irregularities that disturb land vehicles. The tracking ability of the proposed controller design was investigated using various reference inputs with different frequencies. The main contribution of this study is the proposed controller's ability to trace reference signals in both the time and frequency domains concurrently. This dual-domain tracking ability by the controller is a significant advantage, as it allows for more comprehensive and accurate control of systems that have important especially fatigue effects due to the frequency similarities of the real systems to test systems in the laboratory. Moreover, the design of the proposed controller algorithm considers various forces that act within the vehicle system. These include such as spring forces and damping forces. By considering these forces, the controller can more effectively manage the complex dynamics of the vehicle system when it was compared to only hydraulic piston position control algorithms. These considerations ensure that the controller is more applicable to road simulators.

2 Modeling and control of hydraulic system

In this section, two mathematical models will be shown. The first subsection contains the mathematical modeling of the hydraulic system. In the second subsection, the model will be converted to be suitable for applying of the control algorithm.

2.1 Mathematical modeling of hydraulic system

Mathematical modeling of the hydraulic system as shown in Figure 1 can be described by the following equations.

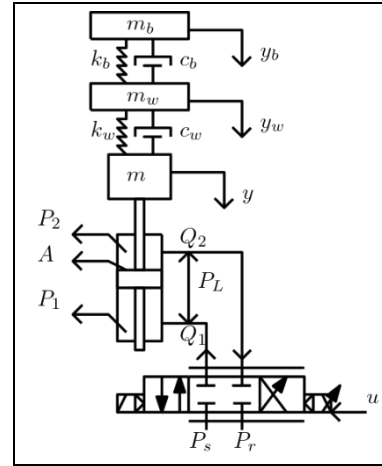


Figure 1. Schematic representation of the hydraulic road test system.

$$\ddot{y}_b = \frac{1}{m_b} (-k_b y_b - c_b \dot{y}_b + k_b y_w + c_b \dot{y}_w) \quad (1)$$

$$\ddot{y}_w = \frac{1}{m_w} (-k_b y_w - c_b \dot{y}_w - k_w y_w - c_w \dot{y}_w + k_b y_b + c_b \dot{y}_b + k_w y + c_w \dot{y}) \quad (2)$$

$$\ddot{y} = \frac{1}{m} (-k_w y - c_w \dot{y} + k_w y_w + c_w \dot{y}_w + A_p P_L) \quad (3)$$

$$\dot{P}_L = -\frac{4\beta_e A_p}{V_t} \dot{y} - \frac{4\beta_e C_{tl}}{V_t} P_L + \frac{4\beta_e C_d w k_i}{V_t \sqrt{\rho}} \sqrt{P_s - (u) P_L} u \quad (4)$$

where y_b, y_w, y are the displacements of the vehicle sections and piston, respectively, and $P_L (P_1 - P_2)$ is the pressure difference in the chambers. The parameter set is explained in Table 1.

Table 1. Definition of Symbols.

Symbol	Definition	Value	Unit
$m_{b,w}$	Vehicle body-wheel masses, piston mass	4500; 300; 125	kg
$k_{b,w}$	Spring coefficients	675709.18; 1471500	N/m
$c_{b,w}$	Damping coefficients	100787.18; 500	Ns/m
A_p	Piston area	0.00539097	m^2
β_e	Bulk modulus	180000000	N/m^2
V_t	Total volume	0.000808646	m^3
C_{tl}	Leakage coefficient	3e-11	-
C_d	Discharge coefficient	0.62	-
w	valve spool gradient	0.024	-
k_i	Gain	3e-4	-
ρ	Density	850	$\frac{kg}{m^3}$
P_s	Pressure	25000000	Pa

2.2 Control problem statement

Tracking of the actual road input signal on the piston displacement can be realized by the designed control input signal after the manipulation of the mathematical equations of the system. The state-space formulation of the system can be written as

$$\begin{aligned} \dot{y}_2 &= \frac{1}{m_b} (-k_b y_1 - c_b y_2 + k_b y_3 + c_b y_4) \cdot \dot{y}_4 \\ &= \frac{1}{m_w} (-k_b y_3 - c_b y_4 - k_w y_3 \\ &\quad - c_w y_4 + k_b y_1 + c_b y_2 + k_w y_5 \\ &\quad + c_w y_6). \end{aligned} \quad (5)$$

$$\begin{aligned} \dot{y}_6 &= \frac{1}{m} (-k_w y_5 - c_w y_6 + k_w y_3 + c_w y_4 + A_p y_7) \cdot \dot{y}_7 \\ &= -\frac{4\beta_e A_p}{V_t} y_6 - \frac{4\beta_e C_{tl}}{V_t} x_7 \\ &\quad + \frac{4\beta_e C_d w k_i}{V_t \sqrt{\rho}} \sqrt{P_s - (u)} y_7 u. \end{aligned}$$

The state arrangement of the state-space representation of the system is described as

$$\begin{aligned} y &= [y_1, y_3, y_5, y_7]^T = [y_b, y_w, y, P_L]^T; \\ [\dot{y}_1, \dot{y}_3, \dot{y}_5]^T &= [y_2, y_4, y_6]^T \end{aligned} \quad (6)$$

In Equation (6), the term y_1 represents the body's displacement (denoted as y_b), y_3 signifies the displacement of the wheel-axle (notated as y_w), y_5 corresponds to the piston's displacement (represented by y), and y_7 is indicative of the pressure difference in the chamber (expressed as P_L). After the rewriting system equations, the control input signal can be designed for the piston displacement to trace the bounded reference road signal.

2.3 Control design

A backstepping controller is designed for the reference tracking problem of the system and its state-space representation is shown in Equation (5). First of all, the tracking error should be defined. The error signal was designed using the reference road signal (y_{5d}) and the piston displacement signal (y_5).

$$e = y_{5d} - y_5 \quad (7)$$

The time derivative of the error between piston displacement and the reference road signal.

$$\dot{e} = \dot{y}_{5d} - \dot{y}_5 \quad (8)$$

$$\dot{e} = \dot{y}_{5d} - y_6 \pm \phi_1 \quad (9)$$

where ϕ_1 is the virtual control signal.

$$z_1 = \phi_1 - y_6 \quad (10)$$

Consider the candidate Lyapunov function as

$$V_1 = \frac{1}{2} e^2 \quad (11)$$

Then

$$\dot{V}_1 = e(\dot{e}) = e(\dot{y}_{5d} - \phi_1 + z_1) \quad (12)$$

The virtual control signal can be designed after obtaining Equation (12).

$$\phi_1 = \dot{y}_{5d} + k_{g1} e \quad (13)$$

Then

$$\dot{V}_1 = -k_{g1} e^2 + e z_1 \quad (14)$$

The convergence of the error signal can be provided if z_1 converges to zero. The next step of designing the control input signal is to minimize the z_1 .

$$z_1 = \dot{y}_{5d} + k_{g1} e - y_6 \quad (15)$$

Then

$$\dot{z}_1 = \dot{y}_{5d} + k_{g1} \dot{e} - \dot{y}_6 \quad (16)$$

where \dot{y}_6 in Equation (5) substitutes in Equation (16).

$$\begin{aligned} \dot{z}_1 &= \dot{y}_{5d} + k_{g1} (\dot{y}_{5d} - \dot{y}_5) \\ &\quad - \left(\frac{1}{m} (-k_w y_5 - c_w y_6 + k_w y_3 \right. \\ &\quad \left. + c_w y_4 + A_p y_7) \right) \pm \frac{A_p}{m} \phi_2 \end{aligned} \quad (17)$$

where ϕ_2 is the virtual control signal.

$$z_2 = \phi_2 - y_7 \quad (18)$$

Consider the second candidate Lyapunov function as

$$V_2 = V_1 + \frac{1}{2} z_1^2 \quad (19)$$

Then

$$\begin{aligned} \dot{V}_2 &= -k_{g1} e^2 + e z_1 \\ &\quad + z_1 \left(\dot{y}_{5d} + k_{g1} (\dot{y}_{5d} - \dot{y}_5) \right. \\ &\quad \left. - \left(-\frac{k_2}{m} y_5 - \frac{c_2}{m} y_6 + \frac{k_2}{m} y_3 + \frac{c_2}{m} y_4 \right) \right. \\ &\quad \left. + \frac{A_p}{m} z_2 - \frac{A_p}{m} \phi_2 \right) \end{aligned} \quad (20)$$

The virtual control signal in Equation (20) is

$$\begin{aligned} \phi_2 = & \frac{1}{l} \left(\dot{y}_{5d} + k_{g1}(\dot{y}_{5d} - \dot{y}_5) \right. \\ & - \left(-\frac{k_2}{m} y_5 - \frac{c_2}{m} y_6 + \frac{k_2}{m} y_3 + \frac{c_2}{m} y_4 \right) \\ & \left. + e + k_{g2} z_1 \right) \end{aligned} \quad (21)$$

Then

$$\dot{V}_2 = -k_{g1}e^2 - k_{g2}z_1^2 + \frac{A_p}{m} z_1 z_2 \quad (22)$$

The convergence of the z_2 should be shown because of the right side of Equation (22). Also, the actual control input signal has not been reached, yet.

Consider the third candidate Lyapunov function as

$$V_3 = V_2 + \frac{1}{2} z_2^2 \quad (23)$$

Then

$$\begin{aligned} \dot{V}_3 = & -k_{g1}e^2 - k_{g2}z_1^2 + \frac{A_p}{m} z_1 z_2 + z_2 \frac{1}{\frac{A_p}{m}} \left(\ddot{y}_{5d} + \right. \\ & k_{g1} \left(\dot{y}_{5d} - \left(-\frac{k_2}{m} y_5 - \frac{c_2}{m} y_6 + \frac{k_2}{m} y_3 + \frac{c_2}{m} y_4 + \frac{A_p}{m} y_7 \right) \right) - \\ & \left(-\frac{k_2}{m} y_6 - \frac{c_2}{m} \left(-\frac{k_2}{m} y_5 - \frac{c_2}{m} y_6 + \frac{k_2}{m} y_3 + \frac{c_2}{m} y_4 + \frac{A_p}{m} y_7 \right) + \right. \\ & \frac{k_2}{m} y_4 + \frac{c_2}{m} \left(-\frac{k_1}{m_w} y_3 - \frac{c_1}{m_w} y_4 - \frac{k_2}{m_w} y_3 - \frac{c_2}{m_w} y_4 + \frac{k_1}{m_w} y_1 + \right. \\ & \left. \left. \frac{c_1}{m_w} y_2 + \frac{k_2}{m_w} y_5 + \frac{c_2}{m_w} y_6 \right) \right) + \dot{y}_{5d} - x_6 + k_{g2} \left(\dot{y}_{5d} + \right. \\ & \left. k_{g1}(\dot{y}_{5d} - \dot{y}_6) - \left(-\frac{k_2}{m} y_5 - \frac{c_2}{m} y_6 + \frac{k_2}{m} y_3 + \frac{c_2}{m} y_4 + \right. \right. \\ & \left. \left. \frac{A_p}{m} y_7 \right) \right) - \left(-\frac{4\beta_e A_p}{V_t} y_6 - \frac{4\beta_e C_{tl}}{V_t} y_7 + \right. \\ & \left. \frac{4\beta_e C_d w k_i}{V_t \sqrt{\rho}} \sqrt{P_s - (k_g u)} y_7 u \right) \end{aligned} \quad (24)$$

The real control signal in Equation (24) is

$$\begin{aligned} u = & \frac{1}{\frac{4\beta_e C_d w k_i}{V_t \sqrt{\rho}} \sqrt{P_s - (k_g u)}} \left(-\frac{1}{\frac{A_p}{m}} \left(\ddot{y}_{5d} + k_{g1} \left(\dot{y}_{5d} - \right. \right. \right. \\ & \left. \left. \left(-\frac{k_2}{m} y_5 - \frac{c_2}{m} y_6 + \frac{k_2}{m} y_3 + \frac{c_2}{m} y_4 + \frac{A_p}{m} y_7 \right) \right) - \left(-\frac{k_2}{m} y_6 - \right. \right. \\ & \left. \frac{c_2}{m} \left(-\frac{k_2}{m} y_5 - \frac{c_2}{m} y_6 + \frac{k_2}{m} y_3 + \frac{c_2}{m} y_4 + \frac{A_p}{m} y_7 \right) + \frac{k_2}{m} y_4 + \right. \\ & \left. \frac{c_2}{m} \left(-\frac{k_1}{m_w} y_3 - \frac{c_1}{m_w} y_4 - \frac{k_2}{m_w} y_3 - \frac{c_2}{m_w} y_4 + \frac{k_1}{m_w} y_1 + \right. \right. \\ & \left. \left. \frac{c_1}{m_w} y_2 + \frac{k_2}{m_w} y_5 + \frac{c_2}{m_w} y_6 \right) \right) + \dot{y}_{5d} - y_6 + k_{g2} \left(\dot{y}_{5d} + \right. \\ & \left. k_{g1}(\dot{y}_{5d} - \dot{y}_6) - \left(-\frac{k_2}{m} y_5 - \frac{c_2}{m} y_6 + \frac{k_2}{m} y_3 + \frac{c_2}{m} y_4 + \right. \right. \\ & \left. \left. \frac{A_p}{m} y_7 \right) \right) - \frac{4\beta_e A_p}{V_t} y_6 - \frac{4\beta_e C_{tl}}{V_t} y_7 - k_{g3} z_2 - \frac{A_p}{m} z_1 \end{aligned} \quad (25)$$

Then

$$\dot{V}_3 = -k_{g1}e^2 - k_{g2}z_1^2 - k_{g3}z_2^2 \quad (26)$$

where $k_{g1}, k_{g2}, k_{g3} \in R^+$ are the controller gains. The convergence of the error is provided by the designed control input signal.

3 Results

In this section, the experimental results for the reference road tracking of the hydraulic system with integrated backstepping

controller design were carried out. In this experiment, only a hydraulic piston had been used for the experiment. The parameters of the hydraulic system can be found in Table 1. The apparatus was run at idle. So, there is no vehicle on the top land of the piston. The experimental apparatus was shown in Figure 2.

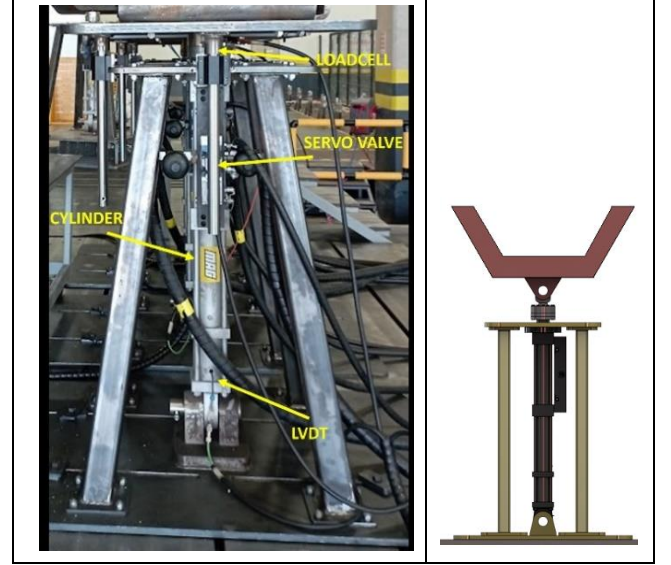


Figure 2. Experimental apparatus.

3.1 Experimental test rig

The experimental rig consists of a hydraulic-piston system with a load cell, two amplifiers, a linear position sensor, two I/O modules, an Industrial PC. (B&R APC 910 controller), a signal amplifier (FUTEK IAA100) for loadcell, an analog input module (B&R X67AI1233), an analog output module (B&R X20AO4632), a signal amplifier (MOOG G123-825-001) and a conditioner for servo valve.

The piston displacement and pressure should be measured to design the full-state feedback controller input signal. The piston displacement was obtained directly by the sensor. The pressures at the piston chambers are accessed over force due to pressure measurement being difficult directly measured by the sensor. The position of the piston is measured by a linear position sensor. The measured position data goes to the I/O module. Simultaneously, the force that is existed due to pressure difference at the chambers, is measured by a load cell. After the force data taken from the load cell goes through an amplifier, enters the I/O module. The load cell and the amplifier provide that the control input signal produced by using these data feeds to the hydraulic valve after the signal goes through another I/O module and a buffer amplifier. The loop is closed by the return of the control signal to the system.

3.2 Experimental results

The experimental results were evaluated in time and frequency domains. In the laboratory environment, tests were performed on the hydraulic piston mechanism as shown in Figure 3. The experiment was performed while the system traced the different road reference inputs. It can be found that 3 different road reference inputs (RRI) have different amplitudes and frequencies in Figure 4.

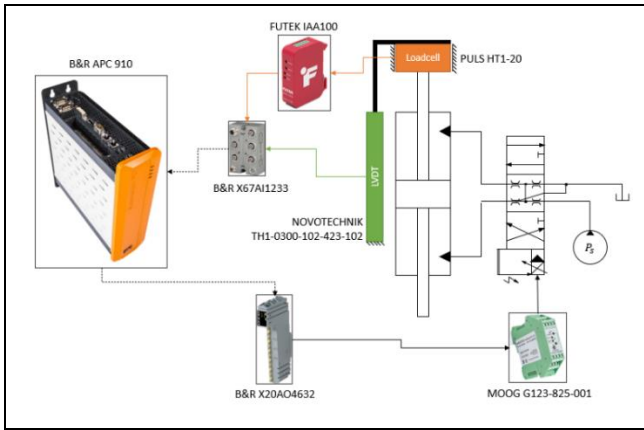
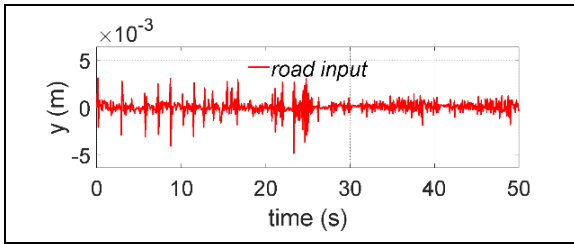
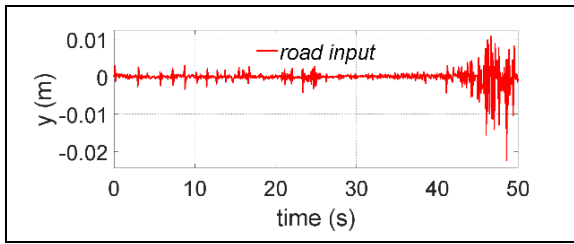


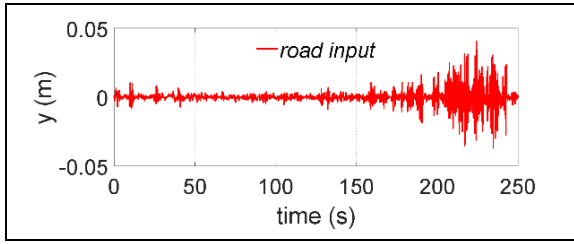
Figure 3. Structure of the test rig.



(a)



(b)



(c)

Figure 4. Road references. (a): RRI 1. (b): RRI 2. (c): RRI 3.

Firstly, the reference road function 1 of the closed loop system's piston displacement was investigated. The comparison during the entrance of the reference signal input 1 to the system was shown in Figure 5, 6, 7.

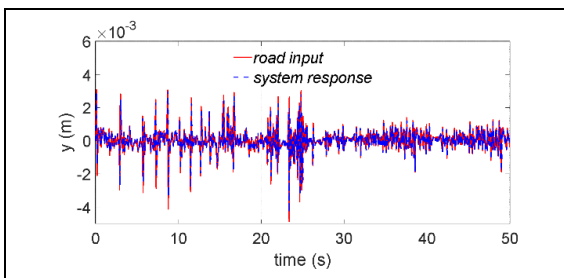


Figure 5. Piston displacement and RRI 1.

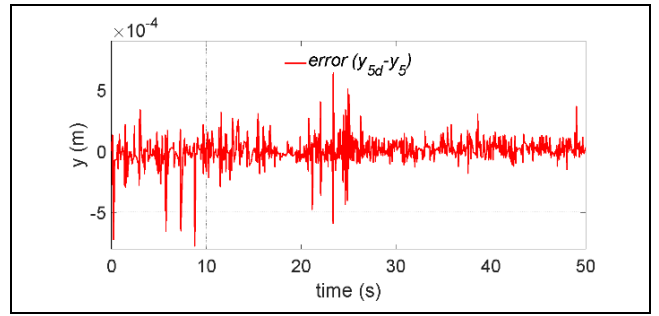
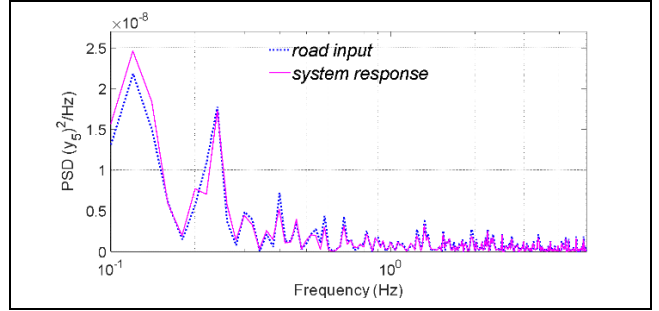
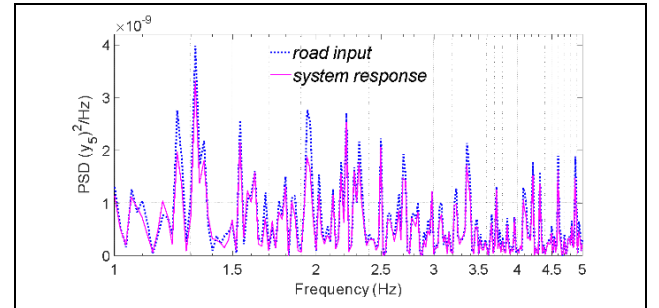


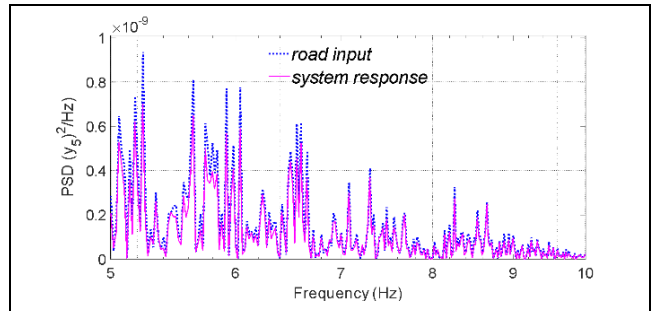
Figure 6. Error between piston displacement and RRI 1.



(a)



(b)



(c)

Figure 7. Piston displacement and RRI 1 (frequency domain). (a): 0.1-10 Hz interval. (b): 1-5 Hz interval. (c): 5-10 Hz interval.

The article's main claim is the achievement of reference tracking in both the time and frequency domains. In Figure 5, the control design ensures great tracking performance in the time domain. However, the frequency response greatly affects fatigue stress [36]. Thus, it should be considered when tracing the road reference. The designed control algorithm was shown a magnificent performance, especially at the low frequency.

To achieve a harder reference input signal, a road function with a bigger amplitude was selected. The responses at the time domain are shown in Figure 8 and Figure 9. In Figure 10, it can be also found the frequency domain response.

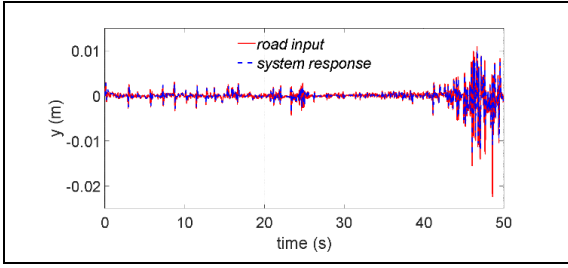


Figure 8. Piston displacement and RRI 2.

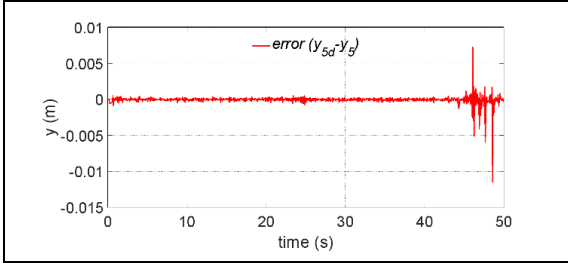
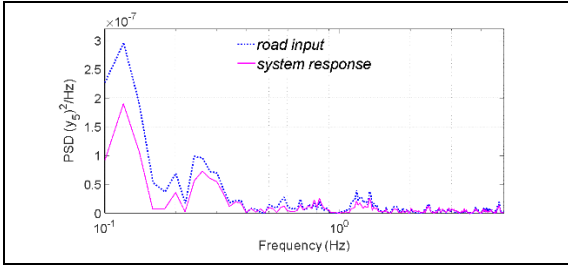
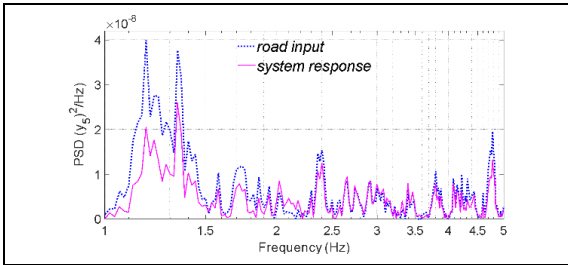


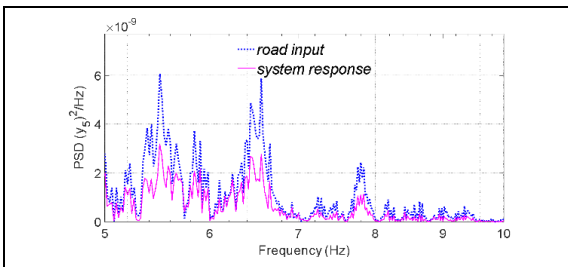
Figure 9. Error between piston displacement and RRI 2.



(a)



(b)



(c)

Figure 10. Piston displacement and RRI 2(frequency domain).
(a): 0.1-10 Hz interval. (b): 1-5 Hz interval. (c): 5-10 Hz interval.
The proposed controller design performs well at the reference tracking whose amplitude is less than 1 cm. As seen in Fig. 9, the performance was reduced when the amplitude of the signal was higher. Similarly, the reference tracking performance is poor at higher magnitudes in frequency domain. Despite this hard reference, the designed controller has a good achievement in

less than 5 Hz. Another challenging reference input signal was selected to investigate the difference between the achievement of the reference tracking in the time domain and the frequency domain. The experimental responses can be found in Figure 11, 12, 13.

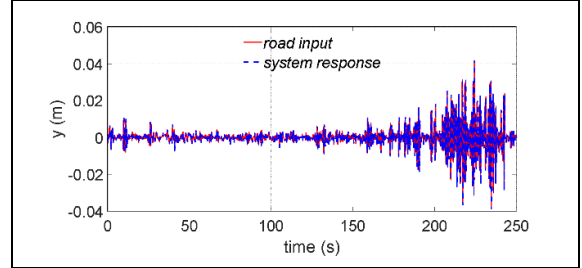


Figure 11. Piston displacement and RRI 3.

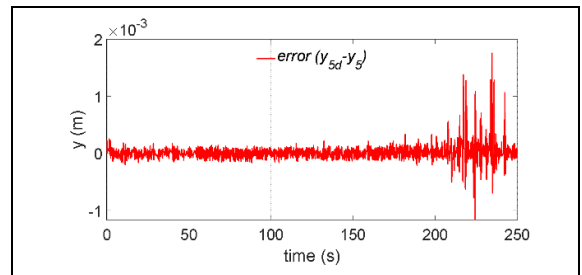
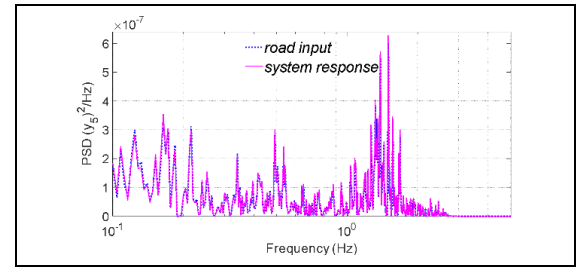
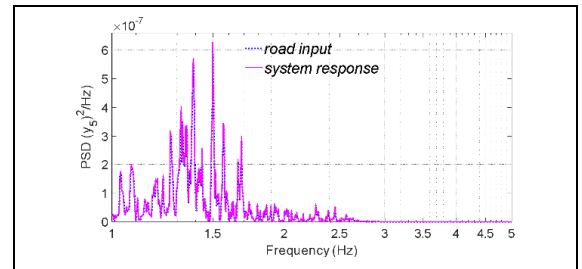


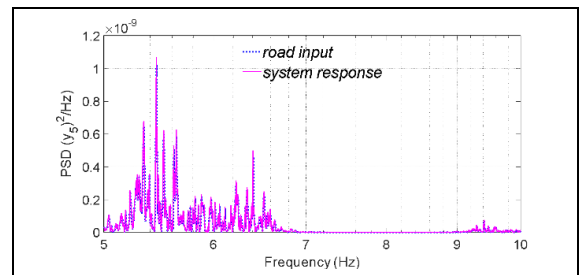
Figure 12. Error between piston displacement and RRI 3.



(a)



(b)



(c)

Figure 13. Piston displacement and RRI 3(frequency domain).
(a): 0.1-10 Hz interval.(b): 1-5 Hz interval. (c): 5- 10 Hz interval.

Figure 11 illustrates the hydraulic piston displacement and reference road signal over time. It can be seen how well and closely the system response (piston displacement) tracks the reference road signal. The error signal in Figure 12 changes over time inside of a limited bound and it can be seen the error signal's amplitude changes depending on the reference signal variations. In Figure 13, the tracking performance of the proposed controller algorithm in the frequency domain can be seen. The tracking ability of the controller is superior.

To understand from another perspective, the ability of the proposed controller at the tracking of the reference road signals, a quantitative comparison between the performance ability of the proposed control algorithm in all scenarios was done with integral square error (ISE), and integral time square error (ITSE). The equation of the ISE, and ITSE performance indices can be seen in Equation (27), and Eq. (28).

$$ISE = \int y^2(t) \quad (27)$$

$$ITSE = \int ty^2(t) \quad (28)$$

In the Equations (27) and (28), y represents of the ISE and ITSE performance indices' variable, it is related with y_5 and y_{5d} in the study. In the Table 2, the results of the performance indices were shown. According to the results, the performance of the proposed controller is satisfactory.

Table 2. Performance Indices.

	ISE		
	$\int y_5^2$	$\int y_{5d}^2$	$\int e^2$
Road Signal 1	1.328e-5	1.606e-5	4.152e-7
Road Signal 2	8.818e-5	1.325e-4	1.373e-5
Road Signal 3	5.408e-3	5.213e-3	4.241e-6
	ITSE		
	$\int ty_5^2$	$\int ty_{5d}^2$	$\int te^2$
Road Signal 1	2.568e-4	3.008e-4	6.873e-6
Road Signal 2	3.823e-3	5.878e-3	6.309e-4
Road Signal 3	1.128	1.087	8.720e-4

Based on the experimental results of road signals, it can be concluded that if the signal has a large amplitude or high frequency within the required power, the selected hydraulic piston can produce at its limit. This suggests that the proposed control algorithm is successful in accurately tracking the reference signal.

4 Conclusions

In this paper, a nonlinear position control of the hydraulic valve for the multi-axis fatigue road simulator was developed and successfully applied in a laboratory environment. The backstepping control approach is employed to derive the proposed control algorithm. Experimental results indicate that the control signal exhibits good performance in the time and frequency domains. Furthermore, the reference signal utilized in the control scheme possesses a range of frequency values, rather than a single value, due to its selection as a representation of real road irregularities. These results demonstrate that the proposed controller can be applied to fatigue test systems in the automotive industry.

5 Acknowledgment

The results of this research study, conducted on a real problem in university-industry cooperation, contribute to commercialization. In carrying out the experimental studies,

"Mert Teknik Incorporated, Research and Development Center." and "TIRSAN Trailer Industry and Trade Incorporated, Research and Development Center" contributed.

6 Author contribution statement

In this study, Muzaffer METİN, Fırat Can YILMAZ, Göktürk TAŞAĞİL and Timuçin BAYRAM contributed to improve the idea behind the study. When Muzaffer METİN and Fırat Can YILMAZ design the control algorithm, Timuçin BAYRAM and Göktürk TAŞAĞİL design the test rig. Ferhat YİĞİT obtained the reference actual road signals. Muzaffer METİN controlled the writing, editing, and evaluation of the results.

7 Ethics committee approval and conflict of interest statement

"There is no need to obtain an ethics committee approval in the article prepared".

"There is no conflict of interest with any person/institution in the article prepared".

8 References

- [1] Raath AD, Van Waveren CC. "A time domain approach to load reconstruction for durability testing". *Engineering Failure Analysis*, 5(2), 113-119, 1998.
- [2] Zhidong Y, Yanyan Z, Dacheng C, Yunjia Y. "Iterative approach of tire-coupled road simulator based on singularity threshold criterion". *IEEE 2015 International Conference on Fluid Power and Mechatronics*, Harbin, China, 5-7 August 2015.
- [3] Chindamo D, Gadola M, Marchesin FP. "Reproduction of real-world road profiles on a four-poster rig for indoor vehicle chassis and suspension durability testing". *Advances in Mechanical Engineering*, 9(8), 1-10, 2017.
- [4] Dursun U, Cansever G, Üstoğlu İ. "Neuro-fuzzy iterative learning control for 4-poster test rig". *Transactions of the Institute of Measurement and Control*, 42(12), 2262-2275, 2020.
- [5] Wan KJ, Ji XD, Yi ZJ, Bae KY. "Control system development of the one-axis hydraulic road simulator using QFT". *IEEE 2007 Chinese Control Conference*, Zhangjiajie, China, 26-31 July 2007.
- [6] Anthonis J, Kennes P, Ramon H. "Design and evaluation of a low-power mobile shaker for vibration tests on heavy wheeled vehicles". *Journal of Terramechanics*, 37(4), 191-205, 2000.
- [7] Gizatullin AO, Edge KA. "Adaptive control for a multi-axis hydraulic test rig". *Proceedings of the Institution of Mechanical Engineers, Part I: Journal of Systems and Control Engineering*, 221(2), 183-198, 2007.
- [8] Shen W, Wang JZ, Wang SK. "The control of the electro-hydraulic shaking table based on dynamic surface adaptive robust control". *Transactions of the Institute of Measurement and Control*, 39(8), 1271-1280, 2017.
- [9] Shen G, Lv GM, Ye ZM, Cong DC, Han JW. "Feed-forward inverse control for transient waveform replication on electro-hydraulic shaking table". *Journal of Vibration and Control*, 18(10), 1474-1493, 2012.
- [10] Ayas MS, Sahin E, Altas IH. "High order differential feedback controller design and implementation for a Stewart platform". *Journal of Vibration and Control*, 26(11-12), 976-988, 2020.

- [11] Yao J, Xiao R, Chen S, Di D, Gao S, Yu H. "Acceleration harmonic identification algorithm based on the unscented Kalman filter for shaking signals of an electro-hydraulic servo shaking table". *Journal of Vibration and Control*, 21(16), 3205-3217, 2015.
- [12] Guan GF, Plummer AR. "Acceleration decoupling control of 6 degrees of freedom electro-hydraulic shaking table". *Journal of Vibration and Control*, 25(21-22), 2758-2768, 2019.
- [13] Nedic N, Stojanovic V, Djordjevic V. "Optimal control of hydraulically driven parallel robot platform based on firefly algorithm". *Nonlinear Dynamics*, 82(3), 1457-1473, 2015.
- [14] Dursun U, Üstoğlu İ, Taşçıkaraoğlu FY. "Hidrolik test sisteminin model öngörülmesi kontrolü". *Pamukkale University Journal of Engineering Sciences*, 24(8), 1443-1449, 2018.
- [15] Liu GP, Daley S. "Optimal-tuning nonlinear PID control of hydraulic systems". *Control Engineering Practice*, 8(9), 1045-1053, 2000.
- [16] Liu GP, Daley S, Duan GR. "Application of optimal-tuning PID control to industrial hydraulic systems". *IFAC Proceedings Volumes*, 35(1), 179-184, 2002.
- [17] Onat C, Daşkin M. "Aktif süspansiyon sistemleri için bir elektro-hidrolik eyleyicinin kazanç programlamalı PI kontrolü". *Dicle University Journal of Engineering*, 9(1), 195-203, 2018.
- [18] Çetin Ş, Akkaya AV. "Simulation and hybrid fuzzy-PID control for positioning of a hydraulic system". *Nonlinear Dynamics*, 61(3), 465-476, 2010.
- [19] Phan VD, Vo CP, Dao HV, Ahn KK. "Actuator fault-tolerant control for an electro-hydraulic actuator using time delay estimation and feedback linearization". *IEEE Access*, 9, 107111-107123, 2021.
- [20] Vo CP, Dao HV, Ahn KK. "Robust fault-tolerant control of an electro-hydraulic actuator with a novel nonlinear unknown input observer". *IEEE Access*, 9, 30750-30760, 2021.
- [21] Dao HV, Tran DT, Ahn KK. "Active fault tolerant control system design for hydraulic manipulator with internal leakage faults based on disturbance observer and online adaptive identification". *IEEE Access*, 9, 23850-23862, 2021.
- [22] Feng H, Yin C, Cao D. "Trajectory Tracking of an Electro-Hydraulic Servo System With an New Friction Model-Based Compensation". *IEEE/ASME Transactions on Mechatronics*, 28(1), 473-482, 2022.
- [23] Yao Z, Liang X, Jiang GP, Yao J. "Model-Based Reinforcement Learning Control of Electrohydraulic Position Servo Systems". *IEEE/ASME Transactions on Mechatronics*, 28(3), 1446-1455, 2022.
- [24] Yang G, Yao J. "Nonlinear adaptive output feedback robust control of hydraulic actuators with largely unknown modeling uncertainties". *Applied Mathematical Modelling*, 79, 824-842, 2020.
- [25] Zheng J, Yao J. "Robust adaptive tracking control of hydraulic actuators with unmodeled dynamics". *Transactions of the Institute of Measurement and Control*, 41(14), 3887-3898, 2019.
- [26] Zaare S, Soltanpour MR. "Optimal robust adaptive fuzzy backstepping control of electro-hydraulic servo position system". *Transactions of the Institute of Measurement and Control*, 44(6), 1247-1262, 2022.
- [27] Yao J, Wang X, Hu S, Fu W. "Adaline neural network-based adaptive inverse control for an electro-hydraulic servo system". *Journal of Vibration and Control*, 17(13), 2007-2014, 2011.
- [28] Ahn KK, Nam DNC, Jin M. "Adaptive backstepping control of an electrohydraulic actuator". *IEEE/ASME Transactions on Mechatronics*, 19(3), 987-995, 2013.
- [29] Yang G, Yao J. "Output feedback control of electro-hydraulic servo actuators with matched and mismatched disturbances rejection". *Journal of the Franklin Institute*, 356(16), 9152-9179, 2019.
- [30] Kim W, Won D, Shin D, Chung CC. "Output feedback nonlinear control for electro-hydraulic systems". *Mechatronics*, 22(6), 766-777, 2012.
- [31] Deng W, Yao J, Wang Y, Yang X, Chen J. "Output feedback backstepping control of hydraulic actuators with valve dynamics compensation". *Mechanical Systems and Signal Processing*, 158, 107769, 2021.
- [32] Ba DX, Dinh TQ, Bae J, Ahn KK. "An effective disturbance-observer-based nonlinear controller for a pump-controlled hydraulic system". *IEEE/ASME Transactions on Mechatronics*, 25(1), 32-43, 2019.
- [33] Li S, Guo Q, Yan Y, Shi Y. "Terminal sliding mode observer based-asymptotic tracking control of electro-hydraulic systems with lumped uncertainties". *Transactions of the Institute of Measurement and Control*, 45(1), 17-26, 2023.
- [34] Kilic E, Dolen M, Koku AB, Caliskan H, Balkan T. "Accurate pressure prediction of a servo-valve controlled hydraulic system". *Mechatronics*, 22(7), 997-1014, 2012.
- [35] Taşağül G, Başgöl B, Metin M, Bayram T. "Elastomer Karakterizasyon Test Sistemlerinin Modellenmesi ve Parametrik Analizleri". *European Journal of Science and Technology*, 20, 881-889, 2020.
- [36] Zhu X, Jones JW, Allison JE. "Effect of frequency, environment, and temperature on fatigue behavior of E319 cast aluminum alloy: Stress-controlled fatigue life response". *Metallurgical and Materials Transactions A*, 39(11), 2681-2688, 2008.